Acta Biomaterialia xxx (xxxx) xxx

Contents lists available at ScienceDirect

Acta Biomaterialia

journal homepage: www.elsevier.com/locate/actbio

Full length article

Isolation and characterisation of wear debris surrounding failed total ankle replacements

Ashley A Stratton-Powell[a,*], Sophie Williams[a], Joanne L Tipper[a,b], Anthony C Redmond[c,d], Claire L Brockett[a,c]

[a] Institute of Medical and Biological Engineering, School of Mechanical Engineering, University of Leeds, Woodhouse Lane, Leeds LS2 9JT, UK
[b] School of Biomedical Engineering, University of Technology Sydney, Ultimo 2007, Australia
[c] NIHR Leeds Biomedical Research Centre, Leeds Teaching Hospitals NHS Trust, UK
[d] Leeds Institute for Rheumatic and Musculoskeletal Medicine, School of Medicine, University of Leeds, UK

ARTICLE INFO

Article history:
Received 24 September 2022
Revised 18 January 2023
Accepted 20 January 2023
Available online xxx

Keywords:
Total joint replacement
Wear debris
Tribology
Foreign body reactions (Response)
Implant retrieval

ABSTRACT

Aseptic loosening and osteolysis continue to be a short- to mid-term problem for total ankle replacement (TAR) devices. The production of wear particles may contribute to poor performance, but their characteristics are not well understood. This study aimed to determine the chemical composition, size and morphology of wear particles surrounding failed TARs. A recently developed wear particle isolation method capable of isolating both high- and low-density materials was applied to 20 retrieved periprosthetic tissue samples from 15 failed TARs of three different brands. Isolated particles were imaged using ultra-high-resolution imaging and characterised manually to determine their chemical composition, size, and morphology. Six different materials were identified, which included: UHMWPE, calcium phosphate (CaP), cobalt chromium alloy (CoCr), commercially pure titanium, titanium alloy and stainless steel. Eighteen of the 20 samples contained three or more different wear particle material types. In addition to sub-micron UHMWPE particles, which were present in all samples, elongated micron-sized shards of CaP and flakes of CoCr were commonly isolated from tissues surrounding AES TARs. The mixed particles identified in this study demonstrate the existence of a complex periprosthetic environment surrounding TAR devices. The presence of such particles suggests that early failure of devices may be due in part to the multifaceted biological cascade that ensues after particle release. This study could be used to support the validation of clinically-relevant wear simulator testing, pre-clinical assessment of fixation wear and biological response studies to improve the performance of next generation ankle replacement devices.

Statement of significance

Total ankle replacement devices do not perform as well as total hip and knee replacements, which is in part due to the relatively poor scientific understanding of how they fail. The excessive production of certain types of wear debris is known to contribute to joint replacement failure. This is the first study to successfully isolate and characterise high- and low-density wear particles from tissues collected from patients with a failed total ankle replacement. This article includes the chemical composition and characteristics of the wear debris generated by ankle devices, all of which may affect their performance. This research provides clinically relevant reference values and images to support the development of pre-clinical testing for future total ankle replacement designs.

1. Introduction

Total ankle replacement (TAR) surgery has been developing since the 1970s, but despite improvements in biomaterial wear resistance [1,2] and the understanding of ankle anatomy [3], TAR performance remains highly variable [4]. Aseptic loosening and osteolysis continue to be an early to mid-term problem for TAR [5,6],

* Corresponding author.
E-mail address: A.Stratton-Powell@leeds.ac.uk (A.A. Stratton-Powell).

https://doi.org/10.1016/j.actbio.2023.01.051

with the prevalence of osteolysis being as high as 60% at 10 years [7]. This issue, often reported without an established root cause, has led to the early discontinuation of several TAR products with less than 10 years of clinical follow-up [8,9].

The production of wear debris is well understood to be an unwanted by-product of implantable orthopaedic devices. Device designers are challenged with reducing wear as far as possible. Once implanted, devices can wear at any surface throughout the lifetime of the device via a range of mechanisms [10,11]. In general, wear tends to occur at four interfaces: (1) between the two primary bearing surfaces, (2) between a bearing surface wearing against as non-bearing surface, (3) between the primary bearing surfaces articulating interposed third-body particles, and (4) between two non-bearing surfaces articulating with each other [12]. Wear also occurs in the absence of interfacing surfaces via biological degradation and corrosion [13]. Wear at the primary bearing surface is expected by engineers, minimised by design and subsequently confirmed in the pre-clinical testing phase of device development. As a result, *in vitro* studies have repeatedly shown relatively low primary bearing wear rates for TAR [14–16] leading to the belief that this wear mode is not a significant factor affecting short-term TAR performance [17]. A more consistent concern is wear debris produced by other wear modes, often at the bone-implant interface. Standardised, internationally recognised pre-clinical testing protocols for TAR are only available for optimally positioned components simulated using an idealised walking gait cycle without interposed third-body contaminants [18]. Without knowing their origin, quantity or characteristics, wear particles are viewed by some authors as a catalyst for TAR failure, rather than the cause [19], although other authors disagree [20]. Other prominent hypotheses for generalisable TAR failure exist and include: device malalignment [21], fixation coating delamination [22–24], interfacial fluid pressure with micromotion [25] and the presence of unnoticed pre-existing cysts [26]. Replicating TAR failure and the environment in which other wear modes occur is a significant challenge for engineers.

Ultra-high molecular weight polyethylene (UHMWPE) from the bearing insert [19, 27-33] and metals from the substrate and fixation surfaces [19,22,28,32,34], are commonly found in the periprosthetic tissues surrounding TAR. Methodological limitations associated with standard histological analysis prevented precise characterisation of particles in some studies [20,22]. Low resolution imaging and the presence of tissue obscuring the particles can impede a detailed characterisation. For example, Koivu, et al. [22] reported finding small, sharp particles of foreign materials within histiocytes but no further information about the particles was determined. Several sensitive and high-resolution wear particle isolation methods exist (see ISO 17853) [35]. These methods can be used to measure particle chemical composition, size, volume and shape, all of which are important to determine the potential of particles to cause a biological response (e.g. inflammation, toxicity etc) [36]. A limitation of these techniques, however, is that they can only characterise one material type to the submicron scale. One such method was used by Kobayashi, et al. [37] in the first and only study to isolate and characterise UHMWPE wear particles from tissue surrounding TARs. Synovial fluid aspirate samples were analysed. The isolated UHMWPE wear particles were similar in size but different in morphology to those of total knee replacement (TKR) controls; a discrepancy attributed to differences in the biomechanical environments [37]. Kobayashi, et al. [37] focused solely on isolating UHMWPE, but even if other materials were of interest, the conventional methods published in ISO 17853 would not be useful, as they are not designed to isolate multiple material types.

A method to isolate and characterise mixed-material particle populations from individual tissue samples has recently been developed and validated by the authors of this article [38]. Given the perceived relevance of both bearing wear and other wear modes to the failure of TAR, this modified method was applied to tissue samples retrieved from failed TARs. The aim of this study was to identify which materials comprise the wear particle burden surrounding failed TARs and to determine their characteristics. The results were then compared to previously published literature, including the results from a study using the same isolation method for failed total hip replacements (THRs) and TKRs [38].

2. Materials and methods

Ethical approval was obtained from the UK Health Research Authority (ref: 09/H1307/60). Twenty periprosthetic tissue samples were retrieved during revision TAR surgery from 15 patients, all of whom had consented to participate in the study. Anatomical location was not specified precisely, but the majority of tissue samples were taken from inside and surrounding osteolytic lesions. The average patient age at implantation was 63 years (range: 49 to 71) and the average implantation time was 99 months (range: 4 to 168). All patients were male and osteolysis was the only reason for revision recorded (Table 1).

Of the 20 tissue samples, 17 samples were retrieved from surrounding 13 Ankle Evolutive System (AES) TARs (Transysteme, FR), 2 samples were from one Rebalance TAR (Zimmer Biomet, UK) and one sample was taken from one Buechel Pappas TAR (Endotec, US). One of the AES TARs was an initial design iteration (referred to as 1st generation throughout this article) characterised by its removable stem and single layered hydroxyapatite (HA) fixation coating. The other 12 AES TARs were the final design iteration (referred to as 2nd generation devices), which featured a monobloc stem with dual coated titanium-HA fixation surfaces. The Rebalance TAR featured a dual layered fixation surface composed of a titanium alloy coating with a 'Bone Master' HA top layer. The substrate for AES and Rebalance designs are cobalt chromium alloy. The Buechel Pappas TAR featured a ceramic titanium nitride coating on a titanium alloy substrate. All bearing inserts were composed of conventional UHMWPE except for the Rebalance TAR, which featured a vitamin E UHMWPE variant.

2.1. Wear particle isolation method

Tissue samples were stored in formaldehyde (10% v/v) for at least seven days followed by long-term storage in ethanol (70% v/v) at room temperature. Prior to processing, the samples were inspected visually (Fig. 1). In general, the tissue samples were mostly beige in colour and speckled with metallic debris. Two samples featured slivers of bone with large sections of delaminated fixation surface attached (Fig. 1i). Bone cannot be digested effectively without destroying other particle types (e.g., hydroxyapatite) therefore, these samples were not processed.

A modified method capable of isolating UHMWPE and high-density wear particles from the same periprosthetic tissue sample was used. The details of this method are explained in Stratton-Powell, et al. [38]. Only two procedural changes were made. Tissue sample quantity was reduced from 1 g to 0.8 g to increase the effectiveness of the enzymatic digestion. Also, additional care was taken when processing the tissue to reduce contamination from the stainless-steel instruments. In brief, the method featured four key steps: digestion, separation, isolation, and cleansing. The 0.8 g tissue samples were randomly selected and dissected into 1 mm^3 pieces. The tissue was then processed by enzymatic digestion using a 1 $mg.ml^{-1}$ papain mix followed by a 1 $mg.ml^{-1}$ proteinase K mix over four days. Low ($<$1.0 $g.cm^{-3}$) and high density ($>$2.0 $g.cm^{-3}$) materials from the tissue digest were separated using ultracentrifugation, which was followed by two separate processes.

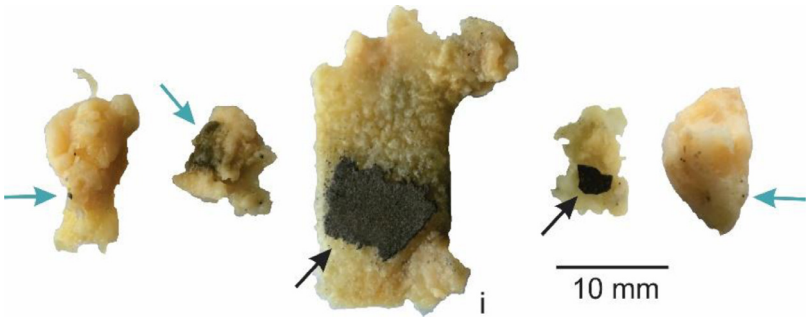

Fig. 1. Examples of tissue samples as received during the retrieval process. Sample (i) was primarily bone and was not processed. Black arrows identify delaminated fixation surface. Blue arrows identify dark coloured debris embedded within the sample.

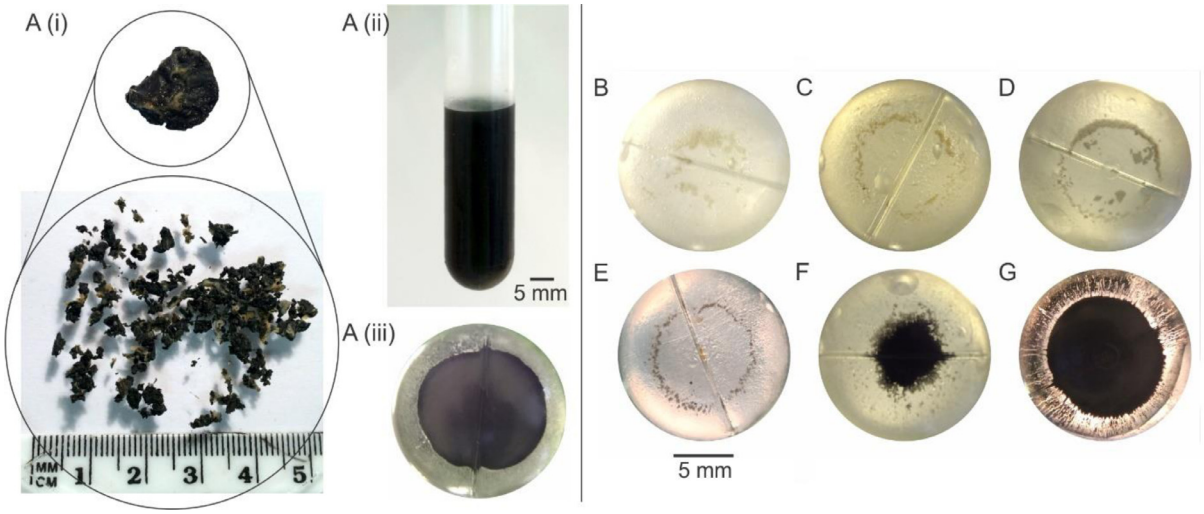

Fig. 2. Photographs of examples of visible wear particle populations from different tissue samples (A-G). A, the periprosthetic tissue sample from a BP TAR which had undergone metal-on-metal contact *in-vivo* (tissue is assumed to be heavily laden with metal particles, hence dark colouration). A(i), tissue sample before and after dissecting. A(ii), wear particles in suspension following cleaning step. A(iii), wear particles following cleaning and centrifugation to allow pellet formation. B-D, visually light off-white particles after isolation. E-G, visually dark metallic particles after isolation. A-G are samples from seven different TARs. Images A(iii) and B-G are photographs of the bottom of the test tube after the final centrifugation step.

Process 1 was used for isolating low density materials, this used a chloroform:methanol mix (2:1) and low speed centrifugation to extract wear particles. Process 2 allowed for isolating high density wear particles using sodium polytungstate density-gradient ultracentrifugation to separate wear particles from the proteinaceous tissue debris. Processes 1 and 2 were modifications of two previously published methods [39,40]. All particle types were washed in their respective processes using centrifugation with ultra-pure water. At this stage, high-density wear particles were often visible at the bottom of the centrifuge tube (Fig. 2). A large volume of metallic wear debris was isolated from the BP TAR tissue sample (Fig. 2A). Visual analysis of the explant suggested the bearing insert had dislocated causing metal-on-metal contact between the tibial and talar bearing surfaces. For all other samples, the wear debris appeared cream/off-white, black or a combination of the two (Fig. 2B–G). Isolated particles were finally extracted by vacuum filtration onto filter membranes with 15 nm pores (GE Whatman, UK) and coated with carbon to a thickness of 5 nm for characterisation.

2.2. Particle characterisation

All filter membranes were imaged using a Hitachi SU8230 high resolution cold-field emission scanning electron microscope (CFE-SEM) with Oxford Instruments Aztec Energy EDX system with 80mm X-Max SDD detector was used at between 50- and 200,000-times magnification. Low density particles were imaged at 2 KV acceleration voltage. A photo diode backscattered electron detector was used at 15 KV acceleration voltage to highlight the presence of high-density materials [41]. Particle chemical composition was identified using energy-dispersive X-ray (EDX) spectroscopy and particle morphology was described qualitatively in accordance with ASTM F1877-16 [42]. Quantitative particle characteristics including major diameter (D_{max}), aspect ratio and roundness were measured manually using ImageJ [43].

2.3. Statistical methods

Non-parametric descriptive statistics were reported for wear particle size (e.g., median size, interquartile range) and parametric descriptive statistics were reported for morphological characteristics (e.g., mean aspect ratio with standard deviation). The proportion of wear particles in the submicron ($<$1 µm), 1 to 10 µm and $>$10 µm size ranges were also recorded. Inferential statistical analyses were not undertaken as this research was exploratory and not driven by a quantitative hypothesis. Data analysis was performed using SPSS Statistics Version 22 (IBM Corp, USA).

3. Results

High- and low-density wear particles were isolated and characterised from at least one tissue sample for each of the 15 revised TARs. Six different materials were identified in particles col-

Table 1
Demographic and device material information associated with the analysed total ankle replacement tissue samples.

TAR	Device	Samples (n)	Side	Sex	Diagnosis	Age (yrs.)	Reason for Revision	Implant Time (mo.)	Device Materials			
									Fixation	Tibial	Insert	Talar
1	AES (1st Gen)	1	Left	Male	OA	55	Osteolysis	145	CaP	CoCr	UHMWPE	CoCr
2	AES (2nd Gen)	1	Left	Male	PTOA	69	Osteolysis	91	CPTi/CaP	CoCr	UHMWPE	CoCr
3	AES (2nd Gen)	3	Right	Male	OA	54	Osteolysis	114	CPTi/CaP	CoCr	UHMWPE	CoCr
4	AES (2nd Gen)	1	Left	Male	OA	70	Osteolysis	101	CPTi/CaP	CoCr	UHMWPE	CoCr
5	AES (2nd Gen)	1	Right	Male	OA	68	Osteolysis	87	CPTi/CaP	CoCr	UHMWPE	CoCr
6	AES (2nd Gen)	1	Left	Male	OA	66	Osteolysis	4	CPTi/CaP	CoCr	UHMWPE	CoCr
7	AES (2nd Gen)	2	Right	Male	NK	NK	Osteolysis	NK	CPTi/CaP	CoCr	UHMWPE	CoCr
8	AES (2nd Gen)	1	Right	Male	OA	71	Osteolysis	109	CPTi/CaP	CoCr	UHMWPE	CoCr
9	AES (2nd Gen)	1	Left	Male	OA	NK	Osteolysis	120	CPTi/CaP	CoCr	UHMWPE	CoCr
10	AES (2nd Gen)	1	Right	Male	PTOA	49	NK	97	CPTi/CaP	CoCr	UHMWPE	CoCr
11	AES (2nd Gen)	1	Right	Male	OA	NK	Osteolysis	NK	CPTi/CaP	CoCr	UHMWPE	CoCr
12	AES (2nd Gen)	2	Left	Male	PTOA	60	Osteolysis	70	CPTi/CaP	CoCr	UHMWPE	CoCr
13	AES (2nd Gen)	1	Left	Male	OA	66	Osteolysis	84	CPTi/CaP	CoCr	UHMWPE	CoCr
14	Beuchel Pappas	1	Left	Male	NK	66	NK*	168	TiN/Ti Alloy	Ti Alloy	UHMWPE	Ti Alloy
15	Rebalance	2	Left	Male	NK	NK	Osteolysis	NK	Ti Alloy/CaP	CoCr	UHMWPE†	CoCr

Notes: TAR, Total Ankle Replacement; AES, Ankle Evolutive System; Gen, Generation; OA, Osteoarthritis; PTOA, Post-traumatic Osteoarthritis; †, Vitamin E variant; NK, Not known; mo., Months; yrs., Years; *, Metal-on-metal contacting components evident from explant. CaP, Calcium Phosphate; CPTi, Commercially pure titanium; TiN, Titanium Nitride; Ti, Titanium; CoCr, Cobalt Chromium Alloy; UHMWPE, Ultra-high Molecular Weight Polyethylene.

lected including: UHMWPE, calcium phosphate, cobalt chromium alloy, commercially pure titanium, titanium alloy and stainless steel (Fig. 3). All tissue samples except one contained more than one material type. At least four different particle materials were isolated from tissue surrounding all 12 AES (2nd Generation) devices. Each isolated material corresponded to the materials of the device it was proximal to, except for two AES (2nd Generation) samples in which nine particles of stainless steel were identified for one, and 13 titanium alloy particles were identified for the other (Table 2).

UHMWPE was the only low-density material detected via process 1 and was the most abundant material identified across all samples. UHMWPE particles were much smaller than high-density particles when compared in aggregate for all samples (Fig. 4). For example, 72% (± 20 SD) of isolated UHMWPE particles were in the submicron size range, whereas only 28% (± 17 SD) of high-density particles were submicron in size. Most high-density materials were in the 1 to 10 μm range (61% ± 19 SD) and both UHMWPE and high-density particles had a similar proportion of particles in the >10um size range, 10% (± 12 SD) and 7% (± 9 SD), respectively.

For all wear particles combined, the median D_{max} was 0.84 μm (IQR = 0.14 – 2.45). The median D_{max} for all low density (i.e., UHMWPE) and all high-density wear particles was 0.15 μm (IQR = 0.06 – 0.69), and 1.67 μm (IQR = 0.91 – 3.43), respectively (Full details in Table 3).

Each material tended to have distinct morphological characteristics which were clearly identified visually. EDX analysis was used for material verification and to rule out contaminants throughout the study. Up to 403 UHMWPE particles (mean = 176; min = 56) were characterised per sample and flakes, fibrils, spheroids, and granules were identified (Fig. 5). The largest individual wear particle across all samples was comprised of UHMWPE, which had a major diameter of 630 μm. This particle was fibrillar with a twisted morphology (Fig. 5a).

Calcium phosphate particles were isolated from all AES TARs (n = 13) and were stratified into two particle morphologies, urchin-like particles (Fig. 6a–c) and shard lathe-like particles (Fig. 6d–f). Both particle types had a crystalline morphology. Shards of CaP were generally micron-sized and appear to have broken off from the larger CaP urchin-like particles, which were typically >10μm. The CaP shards had the highest aspect ratio (3.70 ± 1.89 SD) of all the measured particle types (Fig. 7).

The most frequent metal particles isolated from the AES (2nd Generation) devices were cobalt chromium alloy (n = 432) and commercially pure titanium (n = 236). Cobalt chromium alloy particles presented with flake and stacked sheet morphologies (Fig. 6g–i). These particles were elongated and similar in size to CaP shards (Table 3). Commercially pure titanium particles were typically large granular, irregular shapes with rough or flattened edges (Fig. 6j–l). The commercially pure titanium particles were exclusively found in the AES (2nd Generation) samples. The largest high density wear particle was comprised of commercially pure titanium, measuring 102.89 μm in diameter.

Micron-sized irregular flakes of titanium alloy were the most common particle-type isolated from the BP and Rebalance TAR samples (Fig. 6m–o). Spheroidal titanium nitride coated beads from the BP TAR fixation surface were identified but not in sufficient numbers to characterise quantitatively (Fig. 6m, o). Flake-like cobalt chromium alloy particles (n = 47), similar in morphology to those surrounding the AES TARs, were also identified in the Rebalance TAR samples. The hydroxyapatite coating on the Rebalance TAR was not detected.

For four patients, multiple samples were retrieved during the revision surgery from different locations surrounding the TAR device. While the isolated particles were generally the same chemical

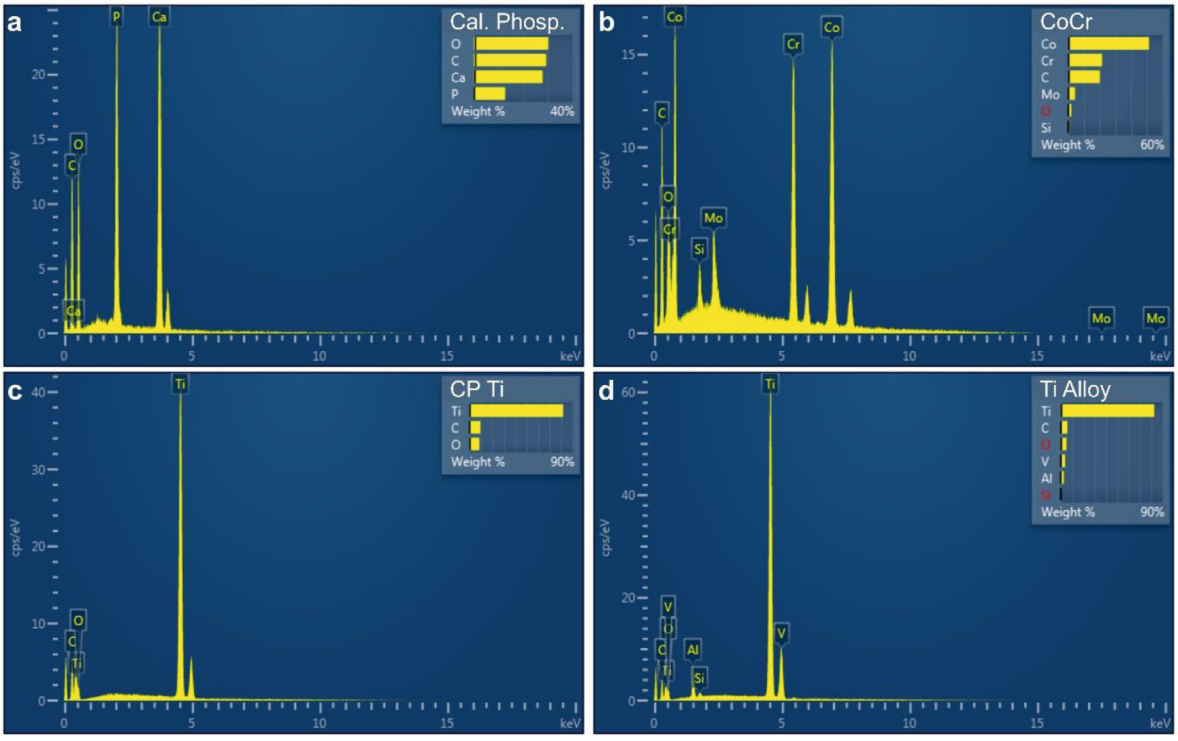

Fig. 3. Examples of energy dispersive X-ray analysis traces for particles isolated from tissue taken at TAR revision showing calcium phosphate (a), cobalt chromium alloy (b), commercially pure titanium (c) and titanium alloy (d).

Table 2
Number and type of isolated wear particles with a comparison between the isolated particle materials and the known explant materials.

TAR	Device	Total	UHMWPE	Calcium Phosphate		CoCr	CPTi	Ti Alloy	SS	Discrepancies between the isolated particle materials and the known explant materials
				Shards	Bulk					
1	AES (1st Gen)	571	190	328	21	32	0	0	0	All materials identified
2	AES (2nd Gen)	322	56	96	127	16	27	0	0	All materials identified
3a	AES (2nd Gen)	321	195	122	0	2	2	0	0	All materials identified
3b		316	155	70	13	70	8	0	0	
3c		318	76	144	51	12	35	0	0	
4	AES (2nd Gen)	132	71	21	19	7	14	0	0	All materials identified
5	AES (2nd Gen)	153	138	1	0	2	12	0	0	All materials identified
6	AES (2nd Gen)	442	403	5	0	29	5	0	0	All materials identified
7a	AES (2nd Gen)	169	169	0	0	0	0	0	0	All materials identified
7b		361	334	3	0	10	14	0	0	
8	AES (2nd Gen)	354	78	181	56	18	21	0	0	All materials identified
9	AES (2nd Gen)	309	163	104	9	12	21	0	0	All materials identified
10	AES (2nd Gen)	495	199	106	47	134	9	0	0	All materials identified
11	AES (2nd Gen)	669	150	418	52	36	0	13	0	Unknown origin of Ti Alloy
12a	AES (2nd Gen)	386	263	107	2	0	14	0	0	All materials identified
12b		348	222	32	19	29	46	0	0	
13	AES (2nd Gen)	282	209	0	1	55	8	0	9	Unknown origin of SS
14	Beuchel Pappas	385	126	0	0	0	0	259	0	All materials identified
15a	Rebalance	329	154	0	0	35	0	140	0	No 'Bone Master' HA Identified
15b		258	171	0	0	12	0	75	0	
Total		6920	3522	1738	417	511	236	487	9	

Notes: Gen, Generation; CaP, Calcium Phosphate; CPTi, Commercially pure titanium; TiN, Titanium Nitride; Ti, Titanium; SS, Stainless Steel; CoCr, Cobalt Chromium Alloy; UHMWPE, Ultra-high Molecular Weight Polyethylene.

composition between samples from the same ankle, the number of particles and their distributions were nonhomogeneous (Fig. 8).

4. Discussion

In this study, a modified particle isolation method was successfully applied to characterise both high- and low-density wear particles from the same TAR tissue sample. Samples from each ankle were found to contain a mixture of wear particle types. UHMWPE particles were isolated from all TAR samples, which is consistent with the intended wear profile of UHMWPE/CoCr bearings. A novel outcome, however, was that the UHMWPE particles were consistently collocated within the tissue samples with metal and calcium phosphate particles, all of which were characterised for the first time using this modified particle isolation method. The mixed particles identified in this study demonstrate the existence of a

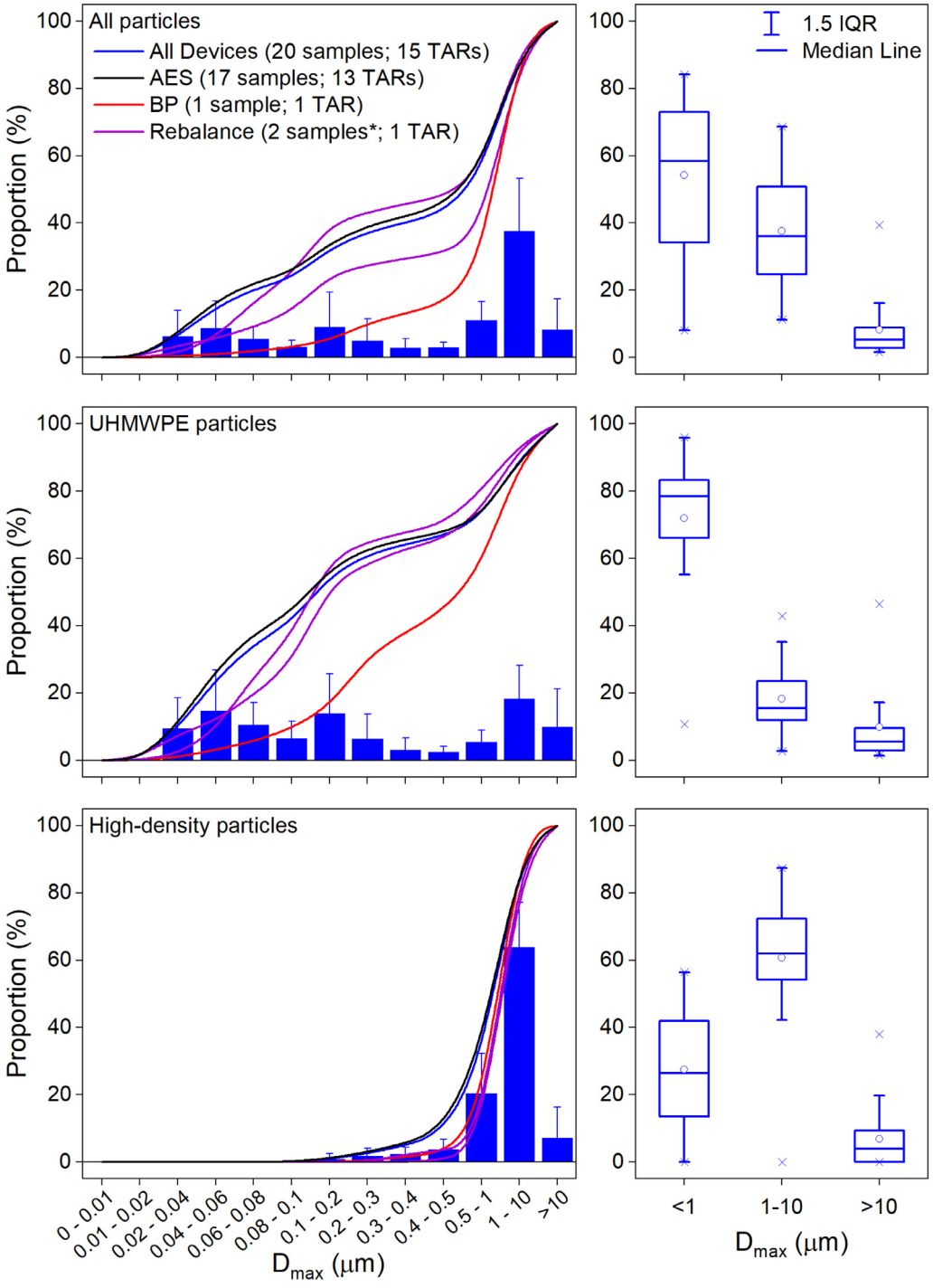

Fig. 4. Size distributions of wear particles isolated from periprosthetic tissue surrounding total ankle replacements (TAR). AES, Ankle Evolutive System; BP, Buechel Pappas; *, The two Rebalance samples are shown; D_{max}, Maximum diameter. IQR, Interquartile range.

complex periprosthetic environment surrounding TAR devices. The presence of such particles suggests that early failure of devices may be due in part to the multifaceted biological cascade that ensues after particle release.

UHMWPE particles produced by THR and TKRs are typically in the submicron size range (~0.1-0.8 µm) [39,44–49], but nanometre-sized granules [38,39,41] and millimetre-sized fibrils are not uncommon [50,51]. The UHMWPE particles produced by TAR appear to be consistent with those produced by THR and TKR. The authors of this study have previously used the same method to isolate and characterise UHMWPE and high-density wear particles from tissue surrounding failed THRs and TKRs [38]. The size and shape of UHMWPE particles were comparable between TAR, THR and TKR with about 72% of particles being in the submicron size range. The primary differences between TAR, THR and TKR was the larger size and more elongated morphology of the high-density wear particles produced by TAR. For cemented THRs and TKRs, the high-density materials were primarily bone cement and their additives ($BaSO_4$ and ZrO_2) in the form of small spheroidal particles. Whereas, in this current study, sharp needle-like particles such as calcium phosphate and irregular-shaped titanium alloy particles were evident. The different particle types produced by TAR

Table 3
Characteristics of particles isolated from total ankle replacements.

Particle Type	Particle Count	D_{max} (µm) Median (Q1, Q3)	Aspect Ratio (Mean ± SD)	Roundness (Mean ± SD)
All Particles	6909	0.84 (0.14, 2.45)	2.23 ± 1.50	0.58 ± 0.23
Max/Min		630.20 / 0.02	15.04 / 1.00	1.00 / 0.07
All UHMWPE	3512	0.15 (0.06, 0.69)	1.61 ± 0.75	0.69 ± 0.17
Max/Min		630.20 / 0.02	13.76 / 1.00	1.00 / 0.07
All High Density	3397	1.67 (0.91, 3.43)	2.87 ± 1.78	0.46 ± 0.22
Max/Min		102.89 / 0.09	15.04 / 1.00	1.00 / 0.07
All CaP	2155	1.50 (0.80, 3.12)	3.28 ± 1.91	0.41 ± 0.21
Max/Min		81.33 / 0.09	15.04 / 1.02	0.98 / 0.07
CaP Shards	1738	1.21 (0.70, 2.02)	3.70 ± 1.89	0.34 ± 0.17
Max/Min		16.19 / 0.09	15.04 / 1.04	0.96 / 0.07
CaP Urchins	417	11.58 (5.05, 21.52)	1.56 ± 0.42	0.68 ± 0.14
Max/Min		81.33 / 0.44	3.83 / 1.02	0.98 / 0.26
CoCr	510	1.26 (0.84, 1.97)	2.35 ± 1.16	0.51 ± 0.19
Max/Min		18.72 / 0.26	9.41 / 1.03	0.97 / 0.11
CP. Titanium	236	2.57 (1.33, 5.61)	1.58 ± 0.40	0.66 ± 0.14
Max/Min		102.89 / 0.36	3.54 / 1.02	0.98 / 0.28
Titanium Alloy	487	3.04 (1.85, 5.38)	2.25 ± 1.49	0.58 ± 0.23
Max/Min		48.14 / 0.29	8.36 / 1.00	1.00 / 0.12
Stainless Steel	9	0.89 (0.23, 1.59)	1.62 ± 0.61	0.67 ± 0.18
Max/Min		1.87 / 0.19	3.10 / 1.09	0.92 / 0.32

Notes: D_{max}, Feret's Diameter; SD, Standard deviation; Q, Quartile; UHMWPE, Ultra-high molecular weight polyethylene; CaP, Calcium Phosphate; CoCr, Cobalt Chromium Alloy; CP, Commercially pure.

had a slightly different size distribution. Only 28% of high-density wear particles were in the submicron range for TAR, compared to 51% for THR and 57% for TKR [38]. Although, this is unlikely to have a meaningful impact on biological reactivity because a similar proportion of wear particles (~90%) for all three joint types were in the phagocytosable size range (< 10 µm). This means the majority of the wear particles were likely able to interface with the immune system and be engulfed by immunological cells such as macrophages. If the high incidence of osteolysis recorded for TAR in this current study was associated with the particles produced, then differences in particle characteristics other than particle size, such as particle morphology or chemical composition, may have had a greater impact on the clinical outcome.

Aspect ratio is an indicator of particle shape, which is a factor that might influence bioreactivity [36]. As a rule of thumb, an aspect ratio of 1.0 to 2.39 suggests the particles are globular/spherical, whereas particles with an aspect ratio of between 2.4 and 5 are considered to have elongated/fibrillar morphologies [52,53]. The aspect ratio for high-density wear particles surrounding TAR was greater (2.9 ± 1.8) than those surrounding THRs (1.6 ± 0.7) and TKRs (2.0 ± 1.3) [38]. Particles with a higher aspect ratio are generally considered to be more biologically reactive [36,52], especially needle-like calcium phosphate crystals [54,55]. The evidence linking particle shape to periprosthetic osteolysis, however, is considered to be weak [56]. The production of larger, elongated calcium phosphate, titanium alloy and cobalt chromium alloy wear particles may be a specific problem for TAR currently, but further research is required to determine the repeatability of this finding.

Kobayashi, et al. [37] are the only other research group to have successfully isolated and characterised wear debris from TAR. They focused on isolating UHMWPE from joint aspirates surrounding two TAR brands, the fixed-bearing Agility TAR (n = 4) and the mobile-bearing STAR (n = 11). All patients were asymptomatic with TARs functioning as intended [37]. The mean particle diameter (ECD) for the STAR was 0.82 ± 0.11 µm, which provides a useful comparator because of its mobile bearing design. This average size was approximately 5.5 times larger than the median maximum diameter presented in the current study (median = 0.15 µm). This difference may be attributed to several factors, the most obvious being differences in isolation methodologies. The method used in their study was one of the first repeatable isolation methods developed in the 1990s [46]. However, this technique lacked the ability to capture nanoscale particles due to the use of a 0.1 µm filter membrane. Also, the automated particle analyser used featured micron-range resolution, meaning nanoscale particles would go unmeasured. Such limitations likely artificially increased the average particle size. Care was taken in the current study to avoid similar limitations. A 0.015 µm filter was used to minimise particle losses and manual characterisation with ultra-high resolution was used to characterise individual particles down to 10 nm in size.

The aspect ratio of the UHMWPE wear particles isolated by Kobayashi, et al. [37] from mobile-bearing TARs were similar (1.57 ± 0.05) to the TARs investigated in this current study (1.61 ± 0.75). Notably, the variance was much broader in the current study than for the parameters calculated by Kobayashi, et al. [37]. This may be because each individual particle was manually characterised; therefore, agglomerates were excluded and particles up to 630 µm in size were included. Larger wear particles tended to have flake/irregular forms, whereas nanometre sized particles were typically spheroidal. Characterising the full breadth of particle sizes likely created a broader variance for morphological parameters.

Two or more high-density materials were identified in the tissues surrounding all revised TARs included in this study. The most common type of high-density wear particle isolated from TAR tissue was calcium phosphate. Calcium phosphate particles have been identified in histological studies investigating TAR devices [22,24,57–59] and have been suggested to originate from the hydroxyapatite coating [24,58], surrounding bone [57] or ossifications found within cysts [59]. Given the similarity in elemental composition between hydroxyapatite coatings and bone, it is difficult to differentiate the origin of such wear debris solely using elemental analysis. Urchin-like particles have been suggested to originate from hydroxyapatite coatings due to their crystalline features [60]. The absence of a bone-like architecture has also been used to identify particles of hydroxyapatite coating [24]. The crystalline nature of the calcium phosphate particles isolated in this current study suggests they originated from the HA fixation coating, which is consistent with the lack of calcium phosphate particles in tissue samples from non-HA-coated TAR devices.

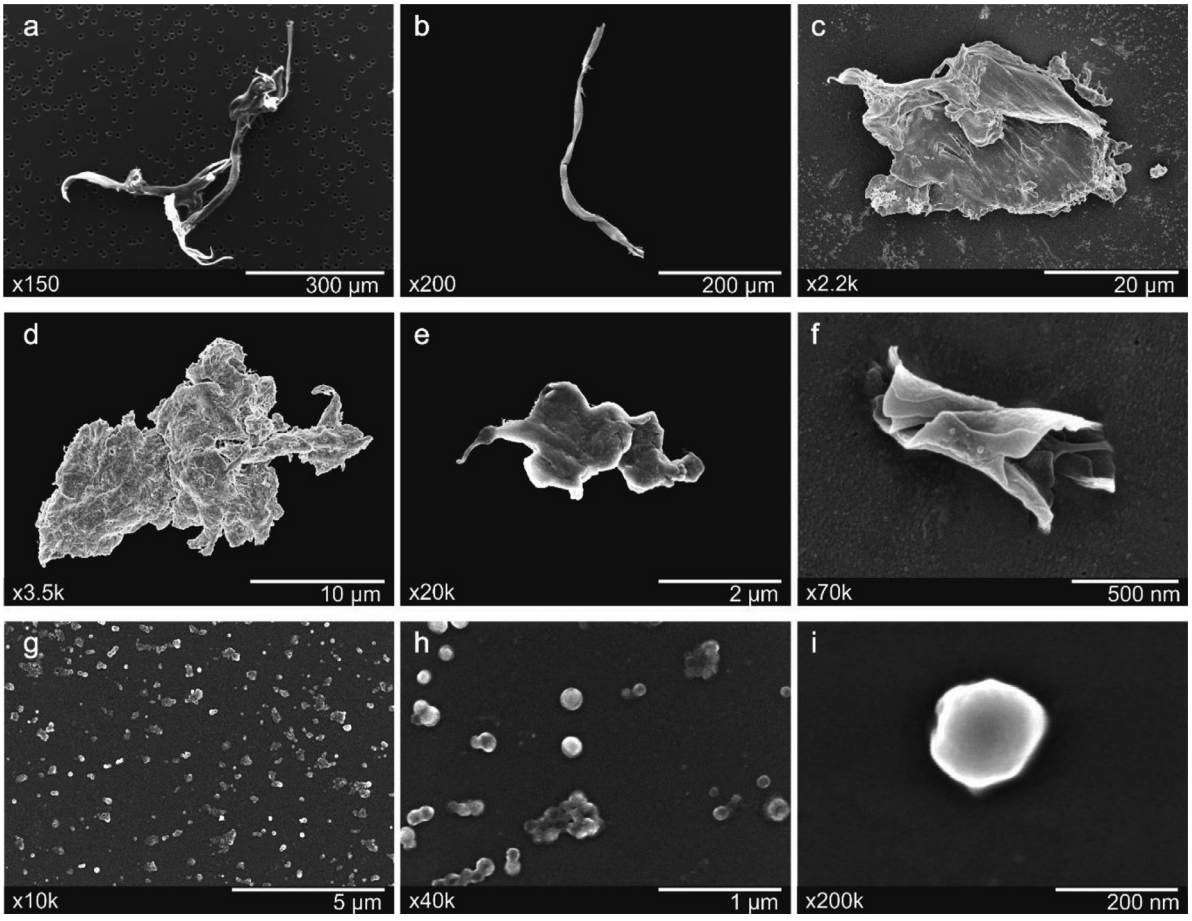

Fig. 5. Ultra-high molecular weight polyethylene wear particle types isolated from periprosthetic tissue surrounding total ankle replacements. A-B, fibrils. C-F, flakes. G-I, granules/spheroids.

Small sharp particles of unknown chemical composition were found previously within histiocytes in AES TAR periprosthetic tissue samples [22]. In a follow-up study, high volumes of necrotic bone fragments were subsequently identified from a similar cohort of patients [57]. Other authors have observed unidentifiable wear particles surrounding TARs, for example Dalat, et al. [58] identified pale particles in the cell cytoplasm, which featured a flaky morphology and were non-birefringent under polarised light. The latter characteristics suggest that the particles were not polymer particles from the bearing surface. The authors of the studies agreed that the disintegration of the fixation surface was likely to produce such particles, but that further analysis of chemical composition was required. The fixation failure hypothesis was later supported when hydroxyapatite coatings from four different TAR devices (STAR, Hintegra, Salto and Taric) were suggested to contribute to osteolysis [24]. Elemental analysis indicated substantial calcium deposits with no bony architecture within the tissue samples [24]. High concentrations of calcium (>0.5 g/g), suggested to have originated from the hydroxyapatite coating, were associated with a 297-fold increased risk of ballooning osteolysis [24]. A mechanistic link, however, was not described, only that high concentrations of calcium were likely associated with the observed osteolysis. All TAR samples processed in this study were from TARs revised for osteolysis. The high prevalence of calcium phosphate particles found in the tissue samples aligns with the previous findings by Singh, et al. [24].

Cobalt chromium alloy and commercially pure titanium wear particles were commonly identified in the AES (2nd Generation) TAR tissue samples and have been identified previously in histological studies for several TAR designs [20,22,24,57–59]. Koivu, et al. [22] reported more titanium wear particles present in their AES TAR tissue samples compared to cobalt chromium particles at 31.3 months follow-up. Singh, et al. [24] found the opposite after measuring more cobalt chromium than titanium at 74 ± 33 months in tissue samples of different TARs using mass spectrometry. Proportionally, more cobalt chromium alloy particles were identified in this current study than titanium particles, with a similar follow-up time to Singh, et al. [24]. Cobalt chromium alloy wear particles in TAR tissue may have originated from the bearing surfaces after fatigue failure and/or third body wear. In such a case, the number of particles produced may be expected to increase as a function of time. Alternatively, cobalt chromium alloy could also have originated at the fixation surface after extensive abrasive wear and/or fixation surface delamination. Fixation surface wear is not unique to TAR, as wear debris indicative of this was identified in several total hip and knee replacement samples using the same isolation method [38]. One key difference, however, is that only 10 cobalt chromium wear particles were identified across the cohort of 18 different hip and knee replacement devices. In this study, 511 cobalt chromium particles were measured. Wear modes other than primary bearing wear, including third body wear, appears to be an issue for the TAR designs included in this study.

Submicron-sized cobalt chromium alloy and titanium wear particles are suggested to contribute to the development of aseptic loosening [61–63]. Cobalt chromium alloy particles produced by metal-on-metal THR articulation tend to be in the nanometre size range [64], whereas particles produced at the fixation surface tend to be larger in size [65]. The difference in particle size is attributed

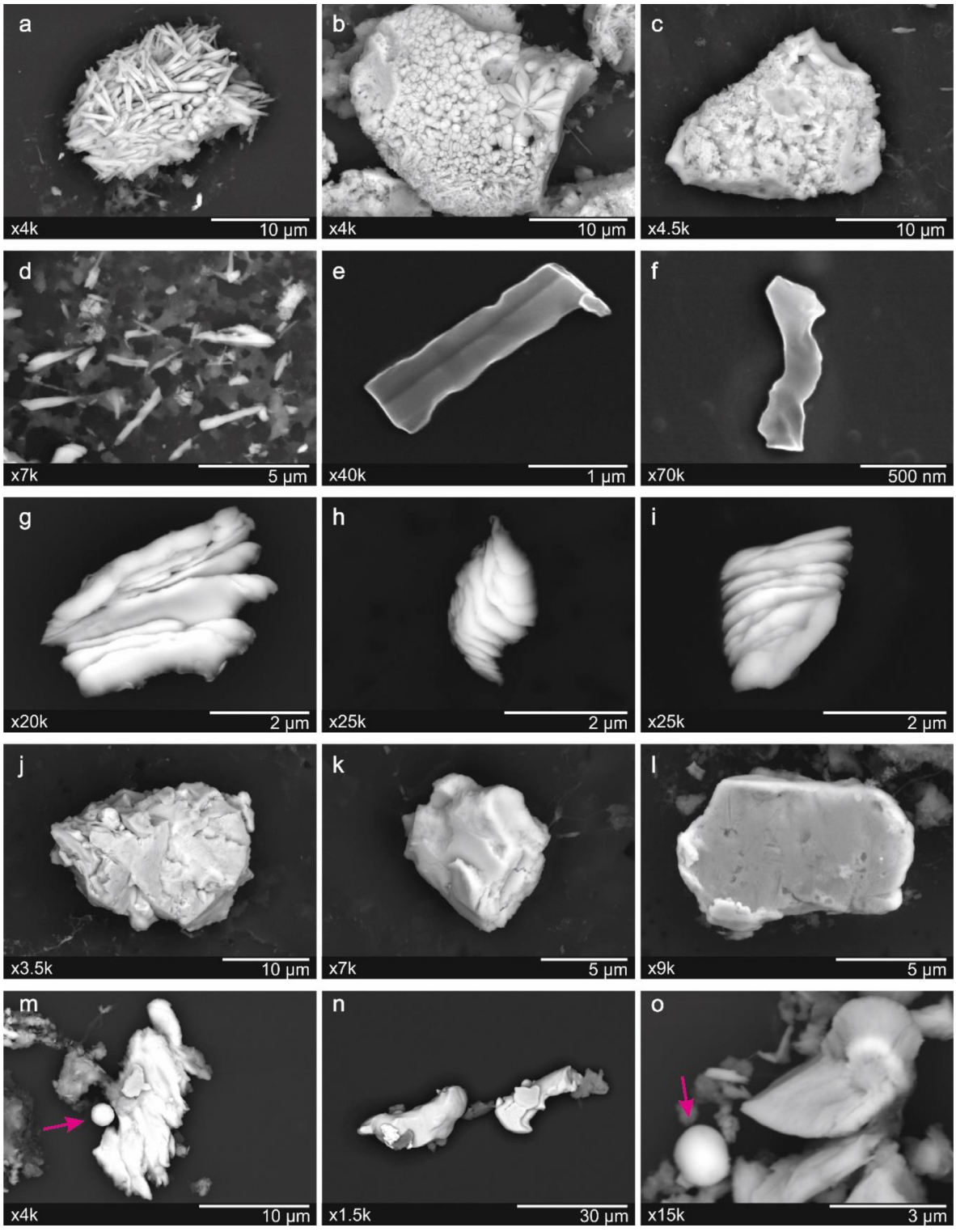

Fig. 6. High density wear particles isolated from periprosthetic tissue surrounding total ankle replacements. a-c, Urchin-like calcium phosphate. d-f, Shard-like calcium phosphate. g-i, Flake-like cobalt chromium alloy. j-l, Commercially pure titanium. m-o, Titanium alloy. Pink arrow, titanium nitride coated fixation beads from the Buechel Pappas TAR.

to different mechanisms of wear, for example fretting versus abrasive wear [66]. Particles with a higher aspect ratio are also considered more biologically reactive [36]. In this current study, both cobalt chromium alloy particles and calcium phosphate particles were within the phagocytosable size-range (<10 μm) and featured high aspect ratios. Further research is required to determine the implications of the identified particle characteristics on biological reactivity.

One AES TAR (1st Generation), one Rebalance TAR (two samples) and one BP TAR were analysed in addition to the 12 AES (2nd Generation) TARs. Each TAR design featured wear particles characteristic of both the fixation surface and substrate materials. Although,

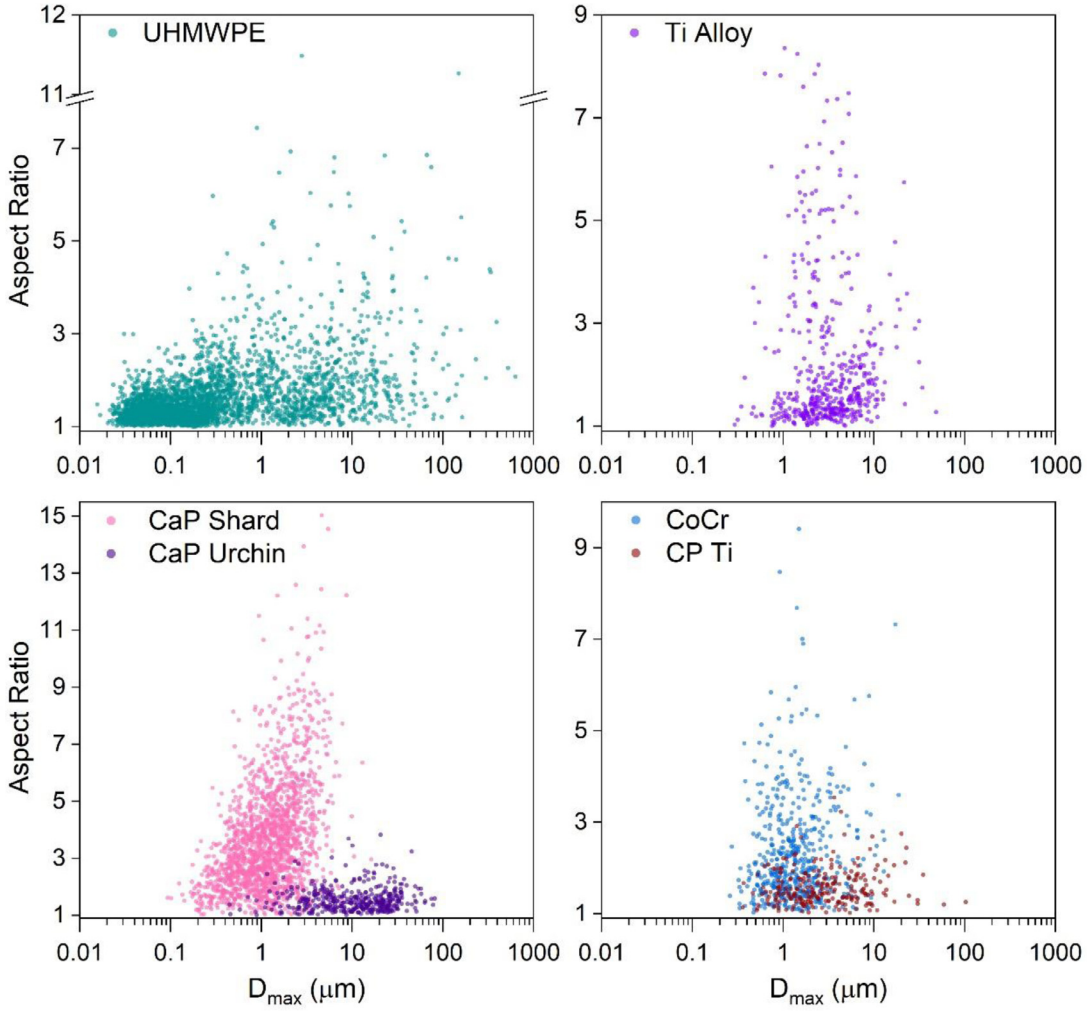

Fig. 7. Particle size and aspect ratio for particle populations isolated from tissues surrounding total ankle replacements. D_{max}, Feret's Diameter; UHMWPE, Ultra-high molecular weight polyethylene; CaP, Calcium Phosphate; CoCr, Cobalt Chromium Alloy; CP Ti, Commercially pure titanium; Ti; Titanium. Note: y-axis varies in magnitude between panels.

the 'Bone Master' HA coating was not detected for the Rebalance TAR in either of the two tissue samples. The titanium alloy wear particles produced by the Rebalance TAR were twice as large as the same particle material produced by the BP TAR. A difference in the wear mechanisms for both TARs is likely the cause for the difference in wear particle size. The Rebalance TAR featured titanium alloy on the fixation surface which was likely abraded by micromotion at the implant-bone interface. The titanium alloy wear particles produced by the subluxed BP TAR were likely to be caused by metal-on-metal contact between the tibial bearing surface and the edge of the talar component following displacement of the bearing insert.

4.1. Limitations

The AES TAR was withdrawn from the UK market in 2012 following a high incidence of subchondral cysts and osteolytic lesions around both the tibial and talar components. Retrieval analysis studies have demonstrated the presence of multiple wear modes affecting the AES TAR [16,67], which is supported by this study from the wear debris identified. Thirteen of the 15 patients recruited for this study had AES TARs, the wear particle profile of which may differ to devices considered to be performing acceptably [37], or devices performing well in idealised conditions such as those tested in simulator studies [68]. The AES device was a performance outlier which may limit the applicability of this research, however, the other two device brands tested in this study have not been subject to recalls and showed a similar trend of mixed wear particle populations in the tissues surrounding the devices after failure.

UHMWPE was characterised by its morphology and, following the exclusion of contaminants (e.g., silica) by EDX analysis, was assumed to be the only material isolated from process 1 (low density materials). It was also challenging to distinguish hydroxyapatite from bone wear particles. Both particle types are composed of calcium phosphate, therefore identification was based on morphology alone. No particles with a bone-like morphology were identified, but this does not exclude the possibility of bone particles being present within the sample.

While the sample size of 20 tissue samples from 15 TARs was acceptable for a particle isolation study, the use of manual characterisation techniques likely caused the relatively high measurement variance observed. The number of particles capable of being measured is orders of magnitude less than for automated particle analysers and manual approaches are labour intensive. The number of samples tested per ankle would ideally have been higher to further investigate the differences in wear particle load between anatomical locations. Heterogeneity in particle distributions

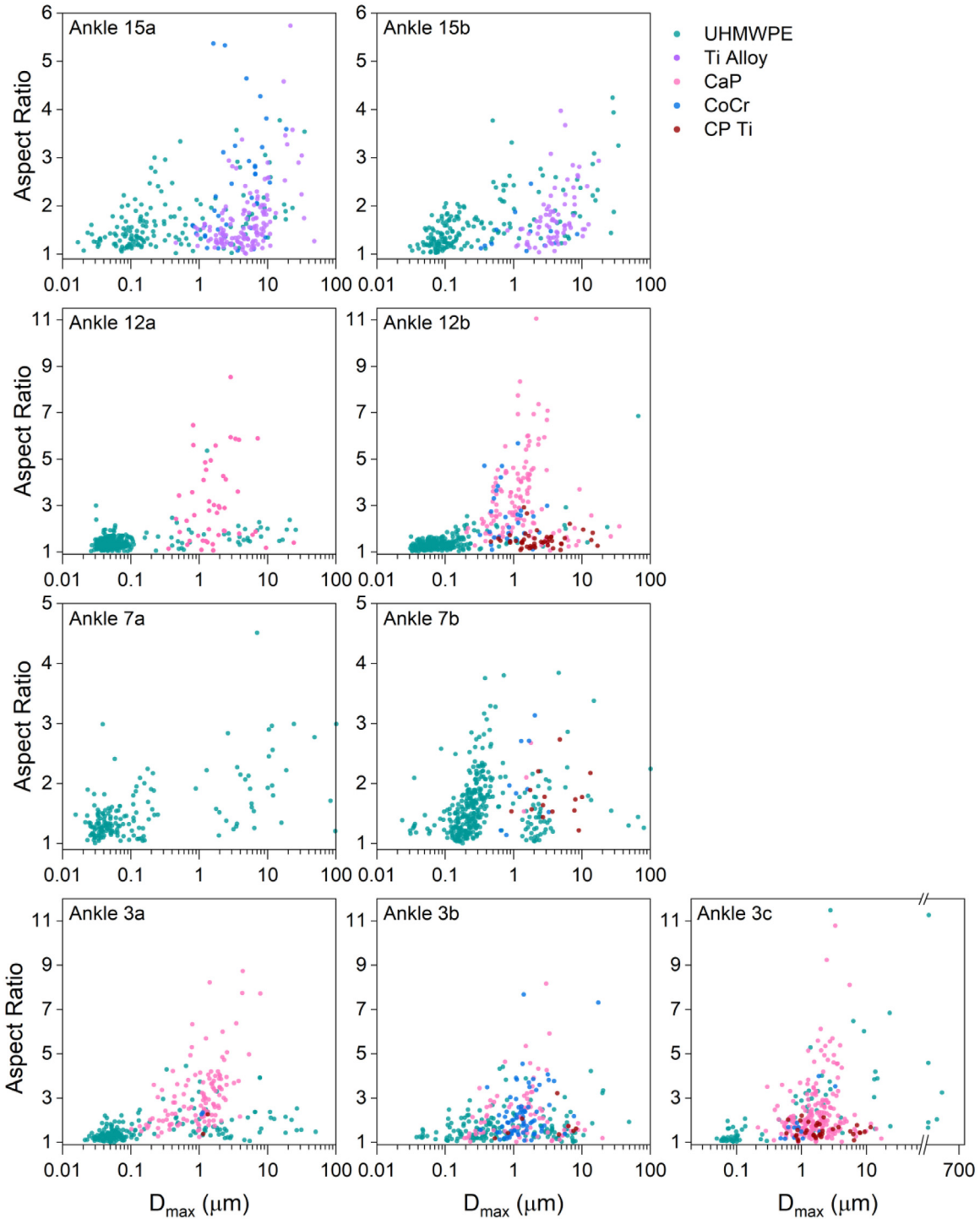

Fig. 8. Particle size and aspect ratio for particle populations isolated from individual tissue samples surrounding four total ankle replacements. Each row represents a different TAR. D_{max}, Feret's Diameter; UHMWPE, Ultra-high molecular weight polyethylene; CaP, Calcium Phosphate; CoCr, Cobalt Chromium Alloy; CP Ti, Commercially pure titanium; Ti; Titanium. Note: y-axis varies in magnitude between panels. Ankle number relates to the sample reference from Table 2.

between anatomical locations is however a known feature of retrieved tissue samples [69].

5. Conclusions

This is the first study to characterise UHMWPE and high-density wear particles from tissues surrounding failed TARs. Tissue samples from each ankle were found to contain a mixture of wear particle types. Submicron UHMWPE particles were repeatably identified and comingled within the tissue samples with particles composed of two or more of the following high-density materials: cobalt chromium alloy, calcium phosphate, titanium alloy, commercially pure titanium and stainless steel. Wear particles suspected to have originated from the fixation surface had a high aspect ratio, which was notably different to wear debris isolated from surrounding cemented THR and TKRs reported in a previous study using the same isolation method. The mixture of particles identified in this study demonstrates the existence of a complex peripros-

thetic environment surrounding TAR devices. Early failure of TAR devices may be due in part to the multifaceted biological cascade that ensues after particle release, particularly from the fixation surface. Further research is needed to understand the total particle burden produced by TAR devices *in-vivo*, particularly the volume of wear. Additionally, broader wear particle characterisation studies are warranted during TAR design and development. The particle images, chemical composition and size data produced in this study can be used to support the validation of clinically-relevant wear simulator testing, pre-clinical assessment of fixation wear and biological response studies to improve the performance of next generation ankle replacement devices.

Data availability statement

The data is openly available via the institutional research data repository for the University of Leeds. This can be accessed using the following DOI: doi.org/10.5518/1277.

Declaration of Competing Interest

None of the authors have conflicts of interest relevant to this research.

Acknowledgments

Funding: This research was funded by the EPSRC Doctoral Training Centre in Tissue Engineering and Regenerative Medicine, a collaboration between the Universities of Leeds, Sheffield, and York [Grant number EP/500513/1]

This research was also supported, in part, by the National Institute for Health Research (NIHR) Leeds Biomedical Research Centre (BRC). The views expressed in this publication are those of the author(s) and not necessarily those of the NIHR, NHS or the UK Department of Health and Social Care.

References

[1] E.T. Davis, J. Pagkalos, B. Kopjar, Effect of bearing surface on survival of cementless and hybrid total hip arthroplasty: study of data in the national joint registry for England, Wales, Northern Ireland and the Isle of Man, JBJS Open Access 5 (2) (2020).
[2] O.N. Schipper, S.L. Haddad, S. Fullam, R. Pourzal, M.A. Wimmer, Wear characteristics of conventional ultrahigh-molecular-weight polyethylene versus highly cross-linked polyethylene in total ankle arthroplasty, Foot Ankle Int. 39 (11) (2018) 1335–1344.
[3] S. Siegler, J. Toy, D. Seale, D. Pedowitz, The clinical biomechanics award 2013 – presented by the International Society of Biomechanics: new observations on the morphology of the talar dome and its relationship to ankle kinematics, Clin. Biomech. 29 (1) (2014) 1–6 (Bristol, Avon).
[4] J.R. Onggo, M. Nambiar, K. Phan, B. Hickey, M. Galvin, H. Bedi, Outcome after total ankle arthroplasty with a minimum of five years follow-up: a systematic review and meta-analysis, Foot Ankle Surg. 26 (5) (2020) 556–563.
[5] J.L. y Hernandez, O. Laffenêtre, E. Toullec, V. Darcel, D. Chauveaux, AKILE™ total ankle arthroplasty: Clinical and CT scan analysis of periprosthetic cysts, Orthop. Traumatol. Surg. Res. 100 (8) (2014) 907–915.
[6] J. Arcângelo, F. Guerra-Pinto, A. Pinto, A. Grenho, A. Navarro, X.Martin Oliva, Peri-prosthetic bone cysts after total ankle replacement. A systematic review and meta-analysis, Foot Ankle Surg. 25 (2) (2019) 96–105.
[7] Y.R.A. Kerkhoff, N.M. Kosse, W.P. Metsaars, J.W.K. Louwerens, Long-term functional and radiographic outcome of a mobile bearing ankle prosthesis, Foot Ankle Int. 37 (12) (2016) 1292–1302.
[8] N. Gougoulias, A. Khanna, N. Maffulli, How successful are current ankle replacements?: a systematic review of the literature, Clin. Orthop. Relat. Res. 468 (1) (2010) 199–208.
[9] H. Koivu, I. Kohonen, K. Mattila, E. Loyttyniemi, H. Tiusanen, Medium to long-term results of 130 Ankle Evolutive System total ankle replacements—Inferior survival due to peri-implant osteolysis, Foot Ankle Surg. (2017).
[10] F. Barrak, S. Li, A. Muntane, M. Bhatia, K. Crossthwaite, J. Jones, Particle release from dental implants immediately after placement – An *ex vivo* comparison of different implant systems, Dent. Mater. 38 (6) (2022) 1004–1014.
[11] Z. Xia, B.F. Ricciardi, Z. Liu, C. von Ruhland, M. Ward, A. Lord, L. Hughes, S.R. Goldring, E. Purdue, D. Murray, G. Perino, Nano-analyses of wear particles from metal-on-metal and non-metal-on-metal dual modular neck hip arthroplasty, Nanomed. Nanotechnol. Biol. Med. 13 (3) (2017) 1205–1217.
[12] H.A. McKellop, The lexicon of polyethylene wear in artificial joints, Biomaterials 28 (34) (2007) 5049–5057.
[13] D.R. Bijukumar, A. Segu, J.C.M. Souza, X. Li, M. Barba, L.G. Mercuri, J.J. Jacobs, M.T. Mathew, Systemic and local toxicity of metal debris released from hip prostheses: a review of experimental approaches, Nanomed. Nanotechnol. Biol. Med. 14 (3) (2018) 951–963.
[14] J.E. Bischoff, J.C. Fryman, J. Parcell, D.A. Orozco Villasenor, Influence of crosslinking on the wear performance of polyethylene within total ankle arthroplasty, Foot Ankle Int. 36 (4) (2015) 369–376.
[15] A. Smyth, J. Fisher, S. Suner, C. Brockett, Influence of kinematics on the wear of a total ankle replacement, J. Biomech. (2017).
[16] S. Affatato, P. Taddei, A. Leardini, S. Giannini, M. Spinelli, M. Viceconti, Wear behaviour in total ankle replacement: a comparison between an *in vitro* simulation and retrieved prostheses, Clin. Biomech. 24 (8) (2009) 661–669 (Bristol, Avon).
[17] J.L. Besse, Osteolytic cysts with total ankle replacement: Frequency and causes? Foot Ankle Surg. 21 (2) (2015) 75–76.
[18] British Standards Institute, BS ISO 22622:2019 Implants for surgery. Wear of total ankle-joint prostheses. Loading and displacement parameters for wear-testing machines with load or displacement control and corresponding environmental conditions for test, 2019.
[19] H. Koivu, Z. Mackiewicz, Y. Takakubo, N. Trokovic, J. Pajarinen, Y. Konttinen, RANKL in the osteolysis of AES total ankle replacement implants, Bone 51 (3) (2012) 546–552.
[20] O.N. Schipper, S.L. Haddad, P. Pytel, Y. Zhou, Histological analysis of early osteolysis in total ankle arthroplasty, Foot Ankle Int. 38 (4) (2017) 351–359.
[21] D. Rodriguez, B.D. Bevernage, P. Maldague, P.A. Deleu, K. Tribak, T. Leemrijse, Medium term follow-up of the AES ankle prosthesis: high rate of asymptomatic osteolysis, Foot and ankle surgery : official journal of the European Society of Foot and, Ankle Surg. 16 (2) (2010) 54–60.
[22] H. Koivu, I. Kohonen, E. Sipola, K. Alanen, T. Vahlberg, H. Tiusanen, Severe periprosthetic osteolytic lesions after the Ankle Evolutive System total ankle replacement, J. Bone Jt. Surg.Br. 91 (7) (2009) 907–914 Volume.
[23] J.L. Besse, N. Brito, C. Lienhart, Clinical evaluation and radiographic assessment of bone lysis of the AES total ankle replacement, Foot Ankle Int. 30 (10) (2009) 964–975.
[24] G. Singh, T. Reichard, R. Hameister, F. Awiszus, K. Schenk, B. Feuerstein, A. Roessner, C. Lohmann, Ballooning osteolysis in 71 failed total ankle arthroplasties: Is hydroxyapatite a risk factor? Acta Orthop. 87 (4) (2016) 401–405.
[25] H.S. Yoon, J. Lee, W.J. Choi, J.W. Lee, Periprosthetic osteolysis after total ankle arthroplasty, Foot Ankle Int. 35 (1) (2014) 14–21.
[26] A.A. Najefi, Y. Ghani, A.J. Goldberg, Bone cysts and osteolysis in ankle replacement, Foot Ankle Int. 42 (1) (2021) 55–61.
[27] V. Valderrabano, B. Hintermann, W. Dick, Scandinavian total ankle replacement: a 3.7-year average followup of 65 patients, Clin. Orthop. Relat. Res. 424 (2004) 47–56.
[28] F. Dalat, R. Barnoud, M.-H. Fessy, J.-L. Besse, Histologic study of periprosthetic osteolytic lesions after AES total ankle replacement. A 22 case series, Orthop. Traumatol. Surg. Res. 99 (6) (2013) S285–S295.
[29] A. Kokkonen, M. Ikavalko, R. Tiihonen, H. Kautiainen, E.A. Belt, High rate of osteolytic lesions in medium-term followup after the AES total ankle replacement, Foot Ankle Int. 32 (2) (2011) 168–175.
[30] N.J. Harris, B.T. Brooke, S. Sturdee, A wear debris cyst following STAR Total Ankle Replacement—surgical management, Foot Ankle Surg. 15 (1) (2009) 43–45.
[31] H.S. Yoon, J. Lee, W.J. Choi, J.W. Lee, Periprosthetic osteolysis after total ankle arthroplasty, Foot Ankle Int. (2013) 1071100713509247.
[32] R. van Wijngaarden, L. van der Plaat, R.A. Nieuwe Weme, H.C. Doets, J. Westerga, D. Haverkamp, Etiopathogenesis of osteolytic cysts associated with total ankle arthroplasty, a histological study, Foot Ankle Surg. 21 (2) (2015) 132–136.
[33] C. Johl, J. Kircher, K. Pohlmannn, V. Jansson, Management of failed total ankle replacement with a retrograde short femoral nail: a case report, J. Orthop. Trauma 20 (1) (2006) 60–65.
[34] G. Singh, T. Reichard, R. Hameister, F. Awiszus, K. Schenk, B. Feuerstein, A. Roessner, C. Lohmann, Ballooning osteolysis in 71 failed total ankle arthroplasties: Is hydroxyapatite a risk factor? Acta Orthop. (2016) 1–5.
[35] British Standard ISO 17853, Wear of implant materials — Polymer and metal wear particles — Isolation and characterization, BS ISO 17853:2011, British Standards Institute, London, UK, 2011.
[36] N.J. Hallab, J.J. Jacobs, Biologic effects of implant debris, Bull. NYU Hosp. Jt. Dis. 67 (2) (2009) 182.
[37] A. Kobayashi, Y. Minoda, Y. Kadoya, H. Ohashi, K. Takaoka, C.L. Saltzman, Ankle arthroplasties generate wear particles similar to knee arthroplasties, Clin. Orthop. Relat. Res. 424 (2004) 69–72.
[38] A.A. Stratton-Powell, S. Williams, J.L. Tipper, A.C. Redmond, C.L. Brockett, Mixed material wear particle isolation from periprosthetic tissue surrounding total joint replacements, J. Biomed. Mater. Res. Part B Appl. Biomater. (2022).
[39] L. Richards, C. Brown, M. Stone, J. Fisher, E. Ingham, J. Tipper, Identification of nanometre-sized ultra-high molecular weight polyethylene wear particles in samples retrieved *in vivo*, J. Bone Jt. Surg. Br. 90 (8) (2008) 1106–1113 Volume.
[40] S. Lal, R. Hall, J. Tipper, A novel method for isolation and recovery of ceramic nanoparticles and metal wear debris from serum lubricants at ultra-low wear rates, Acta Biomater. (2016).
[41] M. Topolovec, I. Milošev, A. Cör, R.D. Bloebaum, Wear debris from hip prostheses characterized by electron imaging, Cent. Eur. J. Med. 8 (4) (2013) 476–484.
[42] ASTM International, F1877–16 Standard practice for characterization of particles, ASTM International,, 2016.

[43] J. Schindelin, I. Arganda-Carreras, E. Frise, V. Kaynig, M. Longair, T. Pietzsch, S. Preibisch, C. Rueden, S. Saalfeld, B. Schmid, Fiji: an open-source platform for biological-image analysis, Nat. Methods 9 (7) (2012) 676–682.
[44] Y. Mochida, T.W. Bauer, T. Koshino, K. Hirakawa, T. Saito, Histologic and quantitative wear particle analyses of tissue around cementless ceramic total knee prostheses, J. Arthroplast. 17 (1) (2002) 121–128.
[45] A.S. Shanbhag, J.J. Jacobs, T.T. Glant, J.L. Gilbert, J. Black, J.O. Galante, Composition and morphology of wear debris in failed uncemented total hip replacement, J. Bone Jt. Surg. Br. 76 (1) (1994) 60–67 Volume.
[46] K.J. Margevicius, T.W. Bauer, J.T. McMahon, S.A. Brown, K. Merritt, Isolation and characterization of debris in membranes around total joint prostheses, J. Bone Jt. Surg. 76 (11) (1994) 1664–1675.
[47] P. Campbell, S. Ma, B. Yeom, H. McKellop, T. Schmalzried, H. Amstutz, Isolation of predominantly submicron-sized UHMWPE wear particles from periprosthetic tissues, J. Biomed. Mater. Res. 29 (1) (1995) 127–131.
[48] M. Visentin, S. Stea, S. Squarzoni, M. Reggiani, C. Fagnano, B. Antonietti, A. Toni, Isolation and characterization of wear debris generated in patients wearing polyethylene Hylamer inserts, gamma irradiated in air, J. Biomater. Appl. 20 (2) (2005) 103–121.
[49] P. Hinarejos, I. Pinol, A. Torres, E. Prats, G. Gil-Gomez, L. Puig-Verdie, Highly crosslinked polyethylene does not reduce the wear in total knee arthroplasty: *in vivo* study of particles in synovial fluid, J. Arthroplast. 28 (8) (2013) 1333–1337.
[50] J. Tipper, E. Ingham, J. Hailey, A. Besong, J. Fisher, B. Wroblewski, M. Stone, Quantitative analysis of polyethylene wear debris, wear rate and head damage in retrieved Charnley hip prostheses, J. Mater. Sci. Mater. Med. 11 (2) (2000) 117–124.
[51] M. Huber, G. Reinisch, G. Trettenhahn, K. Zweymüller, F. Lintner, Presence of corrosion products and hypersensitivity-associated reactions in periprosthetic tissue after aseptic loosening of total hip replacements with metal bearing surfaces, Acta Biomater. 5 (1) (2009) 172–180.
[52] A. Sieving, B. Wu, L. Mayton, S. Nasser, P.H. Wooley, Morphological characteristics of total joint arthroplasty-derived ultra-high molecular weight polyethylene (UHMWPE) wear debris that provoke inflammation in a murine model of inflammation, J. Biomed. Mater. Res. Part A 64 (3) (2003) 457–464.
[53] J.S. Day, D.W. MacDonald, M. Olsen, C. Getz, G.R. Williams, S.M. Kurtz, Polyethylene wear in retrieved reverse total shoulder components, J. Shoulder Elb. Surg. 21 (5) (2012) 667–674.
[54] P. Laquerriere, A. Grandjean-Laquerriere, M. Guenounou, D. Laurent-Maquin, P. Frayssinet, M. Nardin, Correlation between sintering temperature of hydroxyapatite particles and the production of inflammatory cytokines by human monocytes, Colloids Surf. B 30 (3) (2003) 207–213.
[55] P. Laquerriere, A. Grandjean-Laquerriere, E. Jallot, G. Balossier, P. Frayssinet, M. Guenounou, Importance of hydroxyapatite particles characteristics on cytokines production by human monocytes *in vitro*, Biomaterials 24 (16) (2003) 2739–2747.
[56] S.B. Goodman, J. Gallo, Periprosthetic osteolysis: mechanisms, prevention and treatment, J. Clin. Med. 8 (12) (2019) 2091.
[57] H. Koivu, Z. Mackiewicz, Y. Takakubo, N. Trokovic, J. Pajarinen, Y.T. Konttinen, RANKL in the osteolysis of AES total ankle replacement implants, Bone 51 (3) (2012) 546–552.
[58] F. Dalat, R. Barnoud, M.H. Fessy, J.L. Besse, Histologic study of periprosthetic osteolytic lesions after AES total ankle replacement. A 22 case series, Orthop. Traumatol. Surg. Res. 99 (6 SUPPL) (2013) S285–S295.
[59] R. van Wijngaarden, L. van der Plaat, R.A. Nieuwe Weme, H.C. Doets, J. Westerga, D. Haverkamp, Etiopathogenesis of osteolytic cysts associated with total ankle arthroplasty, a histological study, Foot Ankle Surg. 21 (2) (2015) 132–136.
[60] B. Willie, J. Shea, R. Bloebaum, A. Hofmann, Elemental and morphological identification of third-body particulate and calcium stearate inclusions in polyethylene components, J. Biomed. Mater. Res. 53 (2) (2000) 137–142.
[61] A.S. Shanbhag, J.J. Jacobs, J. Black, J.O. Galante, T.T. Glant, Human monocyte response to particulate biomaterials generated *in vivo* and *in vitro*, J. Orthop. Res. 13 (5) (1995) 792–801.
[62] I. Catelas, M.A. Wimmer, S. Utzschneider, Polyethylene and metal wear particles: characteristics and biological effects, Semin. Immunopathol. (2011) 257–271.
[63] J.J. Yao, E.A. Lewallen, W.H. Trousdale, W. Xu, R. Thaler, C.G. Salib, N. Reina, M.P. Abdel, D.G. Lewallen, A.J. van Wijnen, Local cellular responses to titanium dioxide from orthopedic implants, BioResearch Open Access 6 (1) (2017) 94–103.
[64] C. Brown, S. Williams, J.L. Tipper, J. Fisher, E. Ingham, Characterisation of wear particles produced by metal on metal and ceramic on metal hip prostheses under standard and microseparation simulation, J. Mater. Sci. Mater. Med. 18 (5) (2007) 819–827.
[65] W.J. Maloney, R.L. Smith, T.P. Schmalzried, J. Chiba, D. Huene, H. Rubash, Isolation and characterization of wear particles generated in patients who have had failure of a hip arthroplasty without cement, J. Bone Jt. Surg. 77 (9) (1995) 1301–1310.
[66] L. Brown, H. Zhang, L. Blunt, S. Barrans, Reproduction of fretting wear at the stem—cement interface in total hip replacement, Proc. Inst. Mech. Eng. Part H J. Eng. Med. 221 (8) (2007) 963–971.
[67] S. Cottrino, D. Fabregue, A.P. Cowie, J.L. Besse, S. Tadier, L. Gremillard, D.J. Hartmann, Wear study of Total Ankle Replacement explants by microstructural analysis, J. Mech. Behav. Biomed. Mater. 61 (2016) 1–11.
[68] J.E. Bischoff, J.C. Fryman, J. Parcell, D.A. Orozco Villaseñor, Influence of crosslinking on the wear performance of polyethylene within total ankle arthroplasty, Foot Ankle Int. 36 (4) (2015) 369–376.
[69] C.M. Arnholt, J.B. White, J.A. Lowell, M.R. Perkins, W.M. Mihalko, S.M. Kurtz, Postmortem retrieval analysis of metallosis and periprosthetic tissue metal concentrations in total knee arthroplasty, J. Arthroplast. 35 (2) (2020) 569–578.